

Gluing bifurcations in critical flows: The route to chaos in parametrically excited surface waves

Ehud Meron

The James Franck Institute, The University of Chicago, 5640 South Ellis Avenue, Chicago, Illinois 60637

Itamar Procaccia

Department of Chemical Physics, Weizmann Institute of Science, Rehovot 76100, Israel

(Received 30 January 1987)

It is shown that the system of parametrically excited surface waves falls into the class of "critical flows" whose dynamics and transition to chaos can be understood from first-return maps derived in the vicinity of one saddle point in phase space. The onset of chaos is via "gluing bifurcations," which are also common to Lorenz-like flows, but these are intermingled here with usual period-doubling bifurcations. Similar parametrically excited systems might show the full array of routes to chaos which appear in critical flows.

The three "usual" routes to chaos, i.e., period doubling, intermittency, and quasiperiodicity, are ubiquitous in physical systems.¹⁻⁴ Recently, however, it has been stressed that in flows generated by vector fields which possess two homoclinic orbits biasymptotic to a saddle point, one can expect an infinity of other generic scenarios, which appear as the unfolding of a cascade of symmetric gluing bifurcations.⁵⁻⁷ Dynamical systems of this type (hereafter "critical flows") can be analyzed using discontinuous maps of the interval. These maps exhibit both the usual scenarios and others, and were used to unify the renormalization techniques used to calculate universal properties of experimental interest.⁶ Although examples of transitions to chaos in critical flows have been introduced in the context of Rayleigh-Benard convection⁸ and reaction-diffusion systems,⁹ none of these correspond to a concrete experimental system. The aim of this Rapid Communication is to fill this gap.

A case that appears to fall in the relevant class of critical flows is the system of parametrically excited surface waves. An experiment by Ciliberto and Gollub¹⁰ used a cylinder containing water which was mounted on a cone of a loudspeaker, and was oscillated accurately in the vertical direction. When the amplitude of the oscillations exceeded some (frequency-dependent) threshold value, the free surface was deformed by surface waves. The two parameters controlled experimentally are Λ , the amplitude of oscillations, and ω_f , the frequency. A fairly detailed theoretical analysis of this experiment, in the vicinity of a codimension-two point in which the neutral stability curves of two surface modes intersect, was presented in Ref. 11. The theoretical analysis culminated in deriving "amplitude equations" for the time dependence of the competing modes. These were used to rationalize the experimental observations. We shall first show here that the flow induced by these equations is a critical flow, and examine its scenario for the onset of chaos by reducing it to a map of the interval. It turns out that for the experimental setup we do not get "clean" cascades of gluing bifurcations; the usual period-doubling bifurcations interfere with them. Moreover, due to symmetry, we see only one

type of gluing bifurcations. We therefore discuss later some possible modifications of the experimental conditions that can lead to cleaner and richer scenarios. It is noteworthy that with this study we accomplish a complete reduction, hydrodynamic equations, low-dimensional evolution equations, and one-dimensional map, for the system of parametrically excited surface waves.

The evolution equations for the competing modes read¹¹

$$\dot{a} = (-L + i\phi_a)a + i\Gamma_1\bar{a} + i\Gamma_2|a|^2a + i\Gamma_3|b|^2a, \quad (1a)$$

$$\dot{b} = (-L + i\phi_b)b + i\Delta_1\bar{b} + i\Delta_2|b|^2b + i\Delta_3|a|^2b, \quad (1b)$$

where $\phi_{a,b} \propto \omega_{a,b} - \omega_f/2$, ω_a and ω_b being the natural frequencies of the modes, and Γ_1, Δ_1 are proportional to Λ . We recall that to linear approximation the actual amplitude $\zeta_a(t)$ [$\zeta_b(t)$] of the surface deformation is given by the imaginary part of $a(t)e^{it/2}$ [$b(t)e^{it/2}$].

Equations (1) are invariant under the symmetry transformations $(a,b) \rightarrow (-a,b)$, $(a,-b)$, and $(-a,-b)$. Thus any solution which breaks any of these symmetries coexists with its symmetric counterparts. We note that the first two symmetries stem from the rotational symmetry of the fluid system. The nature of the observed flows can be understood from the schematic diagram in Fig. 1. There are three saddle foci in phase space, one at the origin (denoted by O) and the two denoted by S_b^\pm . These two are symmetric under $(a,b) \rightarrow (a,-b)$, and correspond to situations where only the b mode is excited. The coordinates are chosen such that z and x are in the directions of the unstable eigenvectors of O and S_b^\pm , respectively. The coordinates y and s are orthogonal (physically x and y are related to the a mode, whereas z and s are associated with the b mode). In addition, there are four symmetric mixed-mode fixed points of which only the one in the first quadrant, denoted by M , is shown. The latter undergo a Hopf bifurcation leading to limit cycles which grow in size as Λ is raised. A key concept for the understanding of the transition to chaos is that of a *gluing bifurcation*;^{5,7} it refers to a process in which two periodic orbits of periods T_1 and T_2 approach a saddle point, form a pair

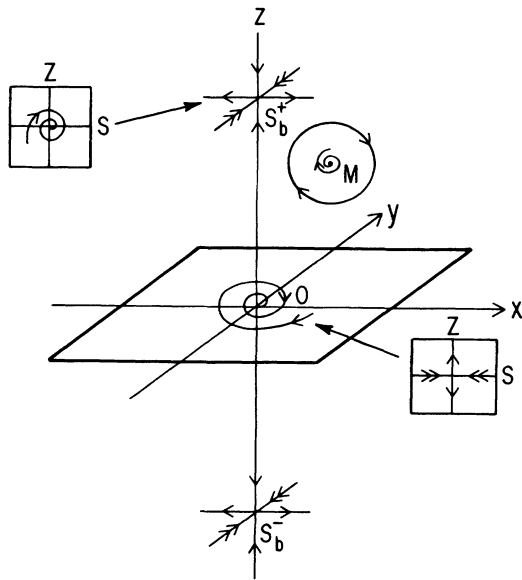


FIG. 1. Fixed points of Eqs. (1) at Λ, ω_f values corresponding to dynamic mode competition.

of homoclinic orbits to that point, and then “glue” together to produce a single periodic orbit of period $T_1 + T_2$. In the present case the invariance of the equations under the transformation $(a, b) \rightarrow (-a, b)$ implies that the glued orbits about S_b^\pm should also be invariant under the transformation. Thus, successive gluing bifurcations may occur only if they are followed by symmetry-breaking ones. In the following we shall consider projections of the flow onto the x - z plane. The transformations $(a, b) \rightarrow (\pm a, \pm b)$ then translate to $(x, z) \rightarrow (\pm x, \pm z)$.

Let us describe now the phenomenology of the transition to chaos as observed by integrating the equations of motion. The transition involves a sequence of gluing bifurcations, the first of which is illustrated in Fig. 2. Notice that both glued and unglued orbits are not symmetric under $(x, z) \rightarrow (x, -z)$. It is only the upper saddle S_b^+ around which all bifurcations occur. The higher bifurcations deform the orbits only in a small neighborhood of S_b^+ . The time signals $x(t)$ reflect these bifurcations most clearly; we can assign to each signal a symbolic se-

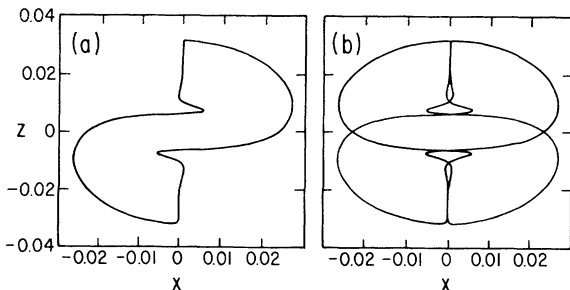


FIG. 2. (a) Gluing of two asymmetric orbits $(R)_\infty$ and $(L)_\infty$, to form (b) a single symmetric $(RL)_\infty$ orbit.

quence by denoting turns to the right (left) of S_b^+ by R (L). Thus, the first bifurcation shown in Fig. 2 corresponds to the gluing of two asymmetric orbits, $(R)_\infty$ and $(L)_\infty$, to form a single $(RL)_\infty$ orbit. The latter has to undergo a symmetry-breaking bifurcation before a successive gluing can take place. This bifurcation is illustrated in Figs. 3(a) and 3(b). The next two gluings and the corresponding symbolic sequences are shown in Figs. 3(c) and 3(d). A closer look at the gluing bifurcations reveals that before gluing the asymmetric orbits undergo a cascade of period-doubling bifurcations. At gluing and in some parameter interval above it the orbit is chaotic. At higher parameter values the glued periodic orbit is recovered. The relative size of the intervals over which chaotic behavior persists grows as the sequence of gluings proceeds and eventually the chaotic motion becomes dominant. A schematic illustration of the transition to chaos is given in Fig. 4.

In critical flows of this type one can gain a better understanding of the transition to chaos by focusing on a first-return map in the vicinity of S_b^+ . In principle, we have a four-dimensional flow and a Poincaré surface of a section should be three dimensional. However, the trajectories of interest pass near O , where s is strongly enslaved by z . As long as x is small, s continues to follow z . As a consequence we find that a section at $z = \text{const}$ yields an effective two-dimensional plane denoted by P . Moreover, we find numerically that orbits intersect this plane such that all intersection points fall on a curve R . We parametrize this curve with a parameter q running between -1 to 1, and compute the first return map $q' = f(q)$. An example is shown in Fig. 5. We note that due to the strong contraction in the y direction (see Fig. 1), the curve

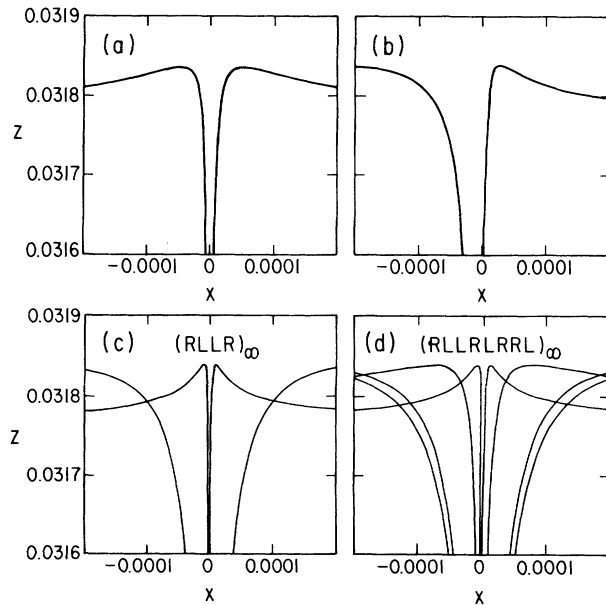


FIG. 3. (a) and (b) A blow up of a small neighborhood around S_b^\pm which shows the symmetry breaking of the $(RL)_\infty$ orbit. (c) and (d) Higher glued orbits and the corresponding symbolic sequences.

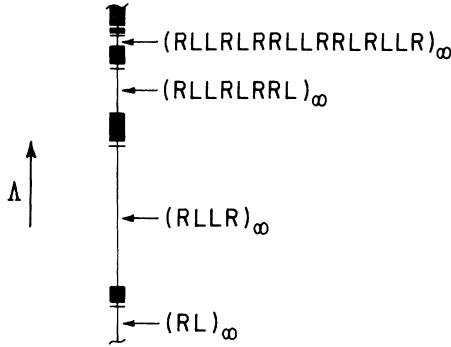


FIG. 4. Schematic illustration of the transition to chaos along a line of constant frequency. White (black) segments correspond to periodic (chaotic) motion. The horizontal bars denote the beginning of period-doubling cascades.

R on P lies very close to the x axis and therefore, to a very good approximation, we can consider the map as acting on that axis. The nature of this map can be understood analytically. The linearized equations around S_b^+ read

$$\dot{x} = \eta_1 x, \quad (2a)$$

$$\dot{y} = -\eta_3 y, \quad (2b)$$

$$\dot{z} = -\eta_2 z + \omega s, \quad (2c)$$

$$\dot{s} = -\eta_2 s - \omega z, \quad (2d)$$

where all the η_i 's are positive and satisfy the inequality $\eta_3 > \eta_1 > \eta_2 > \omega > 0$. Consider now a small neighborhood around S_b^+ within which Eqs. (2) are valid. We rescale the coordinates such that the maps of interest are return maps on the plane $P = \{(x, y, z, s); z = 1, s = 0\}$ and x varies between -1 to 1 . Suppose a trajectory starts at a point $(x_0, y_0, 1, 0)$ on the curve R in P . At time $t^* = -(1/\eta_1) \ln x_0$ it intersects the volume $V = \{(x, y, z, s); x = 1\}$. The coordinates of the intersection point are $(1, y_1, z_1, s_1)$, where

$$y_1 = y_0 x_0^{\eta_3/\eta_1}, \quad (3a)$$

$$z_1 = x_0^{\eta_2/\eta_1} \cos \left[\frac{\omega}{\eta_1} \ln x_0 \right], \quad (3b)$$

$$s_1 = -x_0^{\eta_2/\eta_1} \sin \left[\frac{\omega}{\eta_1} \ln x_0 \right]. \quad (3c)$$

We now expand the x coordinate of the mapped point on P in Taylor series around $(y_1, z_1, s_1) = (0, 0, 0)$. Using the fact the $y_0 \ll x_0$ we obtain the one-dimensional map

$$x' = \begin{cases} -f(x), & x > 0, \\ f(-x), & x < 0, \end{cases} \quad (4a)$$

$$f(x) = f_0 - cx^{\zeta_1} \cos(\zeta_2 \ln x_0 + \psi) + \text{h.o.t.}, \quad (4b)$$

where $\zeta_1 \equiv \eta_2/\eta_1$, $\zeta_2 \equiv \omega/\eta_1$, and h.o.t. represents higher-order terms. We determine the coefficients c and ψ in Eq.

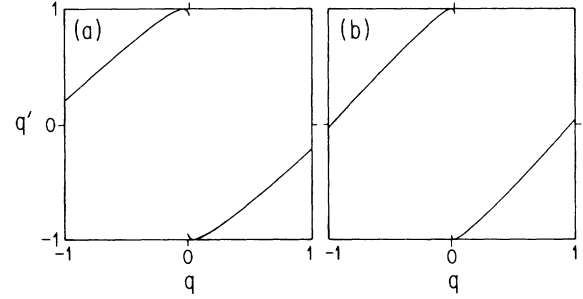


FIG. 5. Numerical first-return maps for (a) the $(RL)_\infty$, and (b) the $(RLLR)_\infty$ orbits. Notice that the map is antisymmetric and nonmonotonic. Gluing occurs when the left and right branches of the map start overlapping.

(4b) by fitting that equation to numerical first return maps evaluated at different Λ values. We find that c is a linear function of f_0 while ψ is constant (specifically, $c = 0.337 + 0.756f_0$ and $\psi = -0.282$). Notice the following. (a) The maps are discontinuous at $x = 0$. This stems from the fact that orbits which start at $x = \pm 0$ follow opposite directions of the unstable manifold. (b) The maps are antisymmetric due to the $(x, y, z, s) \rightarrow (-x, -y, z, s)$ symmetry of the equations of motion. (c) The maps are nonmonotonic in the vicinity of $x = 0$. It is this feature which is responsible for the period-doubling cascade and the subsequent chaotic behavior around gluing. (d) Gluing occurs when the right and left branches of the map start to overlap each other.

The map (4) reproduces accurately the phenomenology described above. It also illuminates the role the eigenvalues of S_b^+ play. The appearance of period-doubling bifurcations and a subsequent chaotic motion stems from the fact that $\zeta_2 \neq 0$ and $\zeta_1 < 1$ (Shil'nicov's condition¹). The former inequality is responsible for the nonmonotonic character of the map. When $\zeta_1 > 1$ the gluing bifurcation is not accompanied by chaotic behavior since the first derivative of the map, $f'(x) \propto x^{\zeta_1-1}$, vanishes as x goes to zero. If, in addition, $\zeta_2 = 0$ or is pure imaginary, complete cascades of gluing bifurcations, characterized by universal numbers which depend on ζ_1 , precede the onset of chaos.^{5,6} Since the eigenvalues of S_b^+ depend on experimental parameters (Λ, ω_f , size and geometry of cell, etc.), all these modifications of the transition to chaos are, in principle, realizable experimentally. Of particular interest is the experimental setup which gives rise to a saddle point with $\zeta_2 = 0$ (or pure imaginary), $\zeta_1 > 1$, and whose rotational symmetry is broken. By breaking the rotational symmetry (working, for example, with an irregularly shaped vessel) one would achieve an *asymmetric* discontinuous first return map. An asymmetric map may also be achieved by exciting a pair of even modes, $a = (2m, 2n)$ and $b = (2n, 2m)$ (or a pair of odd modes) in rectangular geometry.¹¹ This would lead to equations which are not invariant under the transformation $(a, b) \rightarrow (-a, b)$. In such cases one can study the rich variety of codimension-2 routes to chaos which were considered in Ref. 6.

We thank C. Tresser, L. Kadanoff, J. Gollub, and F. Simonelli for useful discussions. This work has been supported in part by the Material Research Laboratory at the University of Chicago. E.M. acknowledges the support of the Dr. Chaim Weizmann Foundation. I.P. acknowledges the support of the Minerva Foundation, Munich, Germany and the Israel Academy of Sciences, the Commission for Basic Research.

-
- ¹J. Guckenheimer and P. Holmes, *Nonlinear Oscillations, Dynamical Systems, and Bifurcations of Vector Fields* (Springer, New York, 1983), and references therein.
- ²A. Libchaber, C. Laroche, and S. Fauve, *J. Phys. (Paris) Lett.* **43**, L211 (1982).
- ³J. Maurer and A. Libchaber, *J. Phys. (Paris) Lett.* **41**, L515 (1980).
- ⁴J. Stavans, F. Heslot, and A. Libchaber, *Phys. Rev. Lett.* **55**, 596 (1985).
- ⁵A. Arneodo, P. Coulet, and C. Tresser, *Phys. Lett.* **81A**, 197 (1981).
- ⁶J.-M. Gambaudo, I. Procaccia, S. Thomae, and C. Tresser, *Phys. Rev. Lett.* **57**, 925 (1986); I. Procaccia, S. Thomae, and C. Tresser, *Phys. Rev. A* **35**, 1884 (1987).
- ⁷J.-M. Gambaudo, P. Glendinning, and C. Tresser (unpublished).
- ⁸J. Coste and N. Peyrand, *Phys. Lett.* **84A**, 17 (1981).
- ⁹Y. Kuramoto and S. Kuga, *Phys. Lett.* **92A**, 1 (1982).
- ¹⁰S. Ciliberto and J. P. Gollub, *Phys. Rev. Lett.* **52**, 922 (1984); *J. Fluid Mech.* **158**, 381 (1985).
- ¹¹E. Meron and I. Procaccia, *Phys. Rev. Lett.* **56**, 1323 (1986); *Phys. Rev. A* **34**, 3221 (1986).